Title: Cytoplasmic protein granules organize kinase-mediated RAS signaling

Authors: Asmin Tulpule[#,1], Juan Guan[#,2,3], Dana S. Neel[#,4], Yone Phar Lin[1], Ann Heslin[1], Hannah R. Allegakoen[1], Shriya Perati[1], Alejandro D. Ramirez[2], Xiaoyu Shi[2], Bin Yang[2], Siyu Feng[5], Suraj Makhija[5], David Brown[2], Bo Huang[2, 6, 7, *], Trever G. Bivona[4,*]

Affiliations:

[1] Division of Pediatric Hematology/Oncology, University of California, San Francisco, San Francisco, CA 94143, USA.

[2] Department of Pharmaceutical Chemistry, University of California, San Francisco, San Francisco, CA 94143, USA.

[3] Department of Physics, University of Florida, Gainesville, FL 32611, USA.

[4] Division of Hematology and Oncology, University of California, San Francisco, San Francisco, CA 94143, USA.

[5] UC Berkeley – UCSF Graduate Program in Bioengineering, University of California, San Francisco, San Francisco, CA 94143, USA.

[6] Department of Biochemistry and Biophysics, University of California, San Francisco, San Francisco, CA 94143, USA.

[7] Chan Zuckerberg Biohub, San Francisco, CA 94158, USA.

*Correspondence to: Trever G. Bivona MD PhD (email: trever.bivona@ucsf.edu) or Bo Huang PhD (email: bo.huang@ucsf.edu)

[#]Equal contribution

Abstract

The spatial organization of a cell includes lipid membrane-based compartments and an emerging class of subcellular structures collectively described as biomolecular condensates[1]. Lipid membranes act as a biologically active scaffold to concentrate signaling molecules in multiple signal transduction pathways that regulate normal physiology and pathologic conditions such as cancer[2]. Notably, receptor tyrosine kinase (RTK)-mediated RAS GTPase/MAP kinase (MAPK) pathway signaling is thought to occur exclusively from lipid membrane compartments in mammalian cells[3,4]. Here, we uncover a membraneless, protein granule-based subcellular structure that can organize RTK/RAS/MAPK signaling. Chimeric (fusion) oncoproteins involving certain RTKs including ALK and RET undergo de novo assembly into cytoplasmic protein granules that locally concentrate the RAS activating complex GRB2/SOS1 and activate RAS in a lipid membrane-independent manner to initiate MAPK signaling. We show that formation of higher-order membraneless protein granules is both necessary and sufficient for RAS/MAPK signaling output in cells. These large-scale protein assemblies are functionally distinct from lower-order oligomerization of cytoplasmic RTK fusion oncoproteins. Our findings reveal membraneless, higher-order cytoplasmic protein assembly as a subcellular platform to

activate RAS GTPases and a distinct principle by which cells can organize kinase-mediated oncogenic signaling.

Main

RTK/RAS/MAPK signaling is broadly important in regulating the proliferation and survival of normal human cells and is often hyper-activated through various mechanisms in human cancer[5]. Evidence of local RAS protein clustering in plasma membrane (PM) microdomains[6,7] and recent reports that the PM resident T-cell receptor and associated proteins undergo phase separation in the presence of lipid bilayers highlight the importance of physical compartmentalization of signaling events[8,9]. Biomolecular condensates are an emerging mechanism of subcellular compartmentalization through primarily protein-based membraneless organelles such as P-bodies, nucleoli and stress granules[10,11]. Though connections between aberrant transcription factor condensates and cancer have been proposed[12,13], the functional role of biomolecular condensates in oncogenic signaling and cancer pathogenesis remains to be defined.

Prominent examples of oncogenic RTK/RAS/MAPK signaling in cancer include chromosomal rearrangements involving RTKs such as anaplastic lymphoma kinase (ALK) or rearranged during transfection (RET), which generate chimeric (fusion) oncoproteins that are validated therapeutic targets across multiple cancer subtypes[14,15]. Virtually all oncogenic ALK fusion proteins retain the intracellular domain, which includes the kinase, but lack the native transmembrane domain[14]. We previously discovered that the echinoderm microtubule-associated protein-like 4 (EML4)-ALK fusion oncoprotein that is present recurrently in lung and other cancer subtypes is exquisitely dependent upon RAS GTPase activation and downstream RAF/MEK/ERK (MAPK pathway) signaling for its oncogenic output[16]. We and other groups showed that EML4-ALK is not localized to the PM, but instead to intracellular, punctate cytoplasmic structures of unknown identity[16,17]. This specific intracellular localization is essential for EML4-ALK to activate RAS and downstream MAPK signaling[16]. Neither the biophysical or biochemical nature of these cytoplasmic structures nor the mechanism through which they promote oncogenic signaling is clear.

To address these knowledge gaps, we focused our initial study on EML4-ALK variant 1, the most common oncogenic form in human cancers[18]. Given the well-established requirement for lipid membranes in mediating RAS GTPase activation[4,19], we first tested whether EML4-ALK localizes to an intracellular lipid membrane-containing structure. Live-cell imaging in a non-transformed human bronchial epithelial cell line (Beas2B) expressing fluorescent protein-tagged EML4-ALK showed no significant colocalization of EML4-ALK cytoplasmic puncta with plasma or intracellular membranes as marked by a membrane intercalating dye, or with a panel of established protein markers labeling canonical intracellular lipid-containing organelles[20] (Extended Data Fig. 1). Additionally, subcellular fractionation in patient-derived cancer cell lines expressing endogenous EML4-ALK protein produced an EML4-ALK fractionation pattern unaffected by membrane-solubilizing detergents, which was distinct from the pattern of PM spanning (epidermal growth factor receptor, EGFR) or internal membrane proteins (calnexin and early endosome antigen 1, EEA1), yet similar to that of a well-known cytoplasmic protein granule constituent (the P-body protein de-capping mRNA 1B, DCP1B[21]) (Fig. 1a, b, and Extended Data Fig. 2). We confirmed by fluorescence microscopy that EML4-ALK puncta do not colocalize with the two known biomolecular condensates in the cytoplasm, P-bodies and stress granules, suggesting EML4-ALK forms distinct membraneless cytoplasmic granules

43 (Extended Data Fig. 1). We validated by immunofluorescence (IF) the similar presence of
44 EML4-ALK cytoplasmic granules in patient-derived cancer cells (H3122) that endogenously
45 express this variant (Fig. 1c) and in human bronchial epithelial cells (Beas2B) expressing FLAG-
46 tagged EML4-ALK (Extended Data Fig. 3a), verifying that these granules were not the result of
47 artificial expression or fluorescent protein-mediated multimerization[22].

48 We further investigated the biophysical nature of EML4-ALK cytoplasmic granules using a suite
49 of established cellular assays to characterize biomolecular condensates[23,24]. During live-cell
50 imaging, no fission or fusion of EML4-ALK granules was observed in spite of occasional
51 granule collisions (Video S1), which is in contrast to the expected behaviors for liquid-like
52 granules. Unlike DCP1B-labelled P-bodies, we found that EML4-ALK granules mostly persist
53 after hexanediol treatment, which disrupts many liquid-like condensates[25] (Extended Data Fig.
54 4). Super-resolution imaging by Structured Illumination Microscopy (SIM) revealed that the
55 EML4-ALK granules exhibit porous and curvilinear features that are distinct from the more
56 uniform appearance of liquid-like granules (Fig. 1d)[10,23]. Moreover, fluorescence recovery after
57 photo-bleaching (FRAP) showed an overall low fraction of exchange of EML4-ALK between
58 the granules and the surrounding cytosol (Fig. 1e). This recovery fraction was heterogeneous
59 amongst granules, varying from 40% to negligible recovery at 1 minute, possibly reflecting an
60 ongoing aging process as maturing granules adopt increasingly solid-like states[24]. EML4-ALK
61 granules are also not disrupted by RNase A, in contrast to ribonucleoprotein granules like the P-
62 body (Extended Data Fig. 5). Taken together, the data indicate EML4-ALK cytoplasmic granules
63 are protein-based instead of RNA-protein-based and demonstrate biophysical properties that are
64 more solid than liquid-like.

65 To uncover the connection between EML4-ALK granules and RAS activation, we created a
66 library of gene-edited Beas2B cell lines by introducing a split mNeonGreen2$_{1\text{-}10/11}$ tag (mNG2) at
67 the endogenous locus of canonical adaptor and effector proteins in the RTK/RAS/MAPK
68 signaling pathway, including GRB2, GAB1, SOS1, and RAS GTPases (H/N/K isoforms)[26]. This
69 suite of isogenic cell lines avoids potential biases that can arise when overexpressing labeled
70 proteins or fixing and permeabilizing cells for immunofluorescence. In this set of cell lines, we
71 found that expression of EML4-ALK specifically re-localized key upstream RAS pathway
72 proteins, including GRB2, GAB1, and SOS1, from a mainly diffusive cytosolic pattern to the
73 discrete EML4-ALK granules (Fig. 1f, g), but not to the PM. This is distinct from the pattern of
74 PM re-localization seen in the control case of expressing an oncogenic form of the
75 transmembrane RTK EGFR (Extended Data Fig. 6). Treatment with the ALK kinase inhibitor
76 crizotinib for 24 hours substantially reduced the recruitment of these adaptor proteins, indicating
77 that this process requires ALK kinase activation (Fig. 1h). We orthogonally confirmed
78 recruitment of the key adaptor, GRB2, both in patient-derived cancer cells and through dual
79 expression of EML4-ALK and GRB2 in Beas2B cells (Fig. 1c and Extended Data Fig. 3b).
80 Additionally, we observed a low and heterogeneous FRAP recovery behavior for GRB2 at the
81 EML4-ALK protein granules, similar to that of EML4-ALK itself (Extended Data Fig. 7).

82 Our imaging and biochemical data prompted the unanticipated hypothesis that RAS GTPase
83 activation may occur via a non-lipid membrane-containing structure (e.g. EML4-ALK
84 membraneless protein granules), potentially through a cytosolic pool of RAS that is known to
85 exist but with unclear functional significance[27]. We first confirmed RAS protein expression in
86 the cytosol where the EML4-ALK granules reside, in addition to lipid membrane subcellular
87 compartments (Extended Data Fig. 8). Next, we directly tested whether cytosolic RAS can

88 become activated in a lipid membrane-independent manner by EML4-ALK protein granules. We
89 utilized established mutant forms of RAS (KRAS-C185S, H/NRAS-C186S) that abrogate lipid
90 membrane targeting and are retained exclusively in the cytosol[19]. While the expression of either
91 EML4-ALK or the PM-localized oncogenic EGFR increased RAS-GTP levels (Fig. 2a and
92 Extended Data Fig. 9), only EML4-ALK increased RAS-GTP levels of cytosolic RAS mutants
93 (Fig. 2b and Extended Data Fig. 9). Furthermore, inhibition of EML4-ALK with crizotinib in
94 H3122 patient-derived cancer cells suppressed not only wild-type RAS-GTP levels, but also the
95 levels of GTP-bound, cytosolic KRAS-C185S (Fig. 2c, d). Control experiments treating a
96 distinct patient-derived cancer cell line HCC827 expressing endogenous oncogenic EGFR (PM-
97 localized) with an established EGFR inhibitor[28] confirmed suppression of wild-type RAS-GTP
98 levels but showed no effect on KRAS-C185S RAS-GTP levels (Extended Data Fig. 10). These
99 findings demonstrate the specificity of cytosolic RAS activation by oncogenic EML4-ALK.

100 Lastly, to determine whether EML4-ALK cytoplasmic granules display evidence of local RAS
101 activation (i.e. RAS-GTP), we used an established tandem GFP-RBD (RAS-binding domain)
102 live-cell reporter given its high affinity binding to RAS-GTP and sensitivity for detection of
103 endogenous RAS activation[29]. When expressed alone, the RAS-GTP reporter displayed
104 homogenous localization in the cytosol and enrichment in the nucleoplasm, as previously
105 described[30] (Fig. 2e). As a positive control, expression of oncogenic KRAS in Beas2B cells led
106 to re-localization of the RAS-GTP reporter to the PM (Extended Data Fig. 11). In EML4-ALK
107 expressing cells, we observed robust enrichment of the RAS-GTP reporter at EML4-ALK
108 cytoplasmic protein granules (Fig. 2e, f) and not at the PM. Co-expression of a dominant
109 negative RAS (RASN17)[31] that interferes with RAS activation (GTP-loading) decreased
110 colocalization of the RAS-GTP reporter at EML4-ALK granules, as did introduction of
111 mutations into the GFP-RBD reporter (R59A/N64D) that decrease affinity for RAS-GTP[29] (Fig.
112 2f). The collective findings show that local RAS activation and accumulation of RAS-GTP
113 occurs at membraneless EML4-ALK cytoplasmic protein granules.

114 We next tested whether downstream MAPK signaling output is dependent on EML4-ALK
115 cytoplasmic protein granules by investigating the molecular determinants of de novo granule
116 formation. The EML4 portion of the chimeric EML4-ALK oncoprotein contains an N-terminal
117 trimerization domain (TD) and a truncated tandem atypical WD-propeller in EML4 protein
118 (TAPE) domain[18] (Fig. 3a). Deletion of the TD or the hydrophobic EML protein (HELP) motif
119 in the propeller domain disrupted protein granule formation, resulting instead in a diffuse
120 cytosolic distribution of EML4-ALK labeled by either fluorescent protein or FLAG-tag (Fig. 3b,
121 c and Extended Data Fig. 12). ΔTD or ΔHELP mutants of EML4-ALK demonstrated loss of
122 ALK trans-phosphorylation and GRB2 interaction (Fig. 3d and Extended Data Fig. 13) and
123 impaired RAS/MAPK activation (Fig. 3e and Extended Data Figs. 13, 14). These data implicate
124 de novo protein granule formation mediated by the EML4 portion of the fusion protein as critical
125 for productive RAS/MAPK signaling. We also observed disrupted granule formation and absent
126 RAS/MAPK signaling with an established kinase-deficient mutant (K589M) form of EML4-
127 ALK (Fig. 3b-e and Extended Data Figs. 12-14), an effect that may be due to phosphorylation
128 events regulating EML4-ALK granule formation, as shown in other protein granule systems[32,33].

129 Our findings prompted a model in which higher-order clustering of an RTK in membraneless
130 cytoplasmic protein granules is sufficient to organize activation of RAS/MAPK signaling. To
131 directly test this hypothesis, we utilized the HOtag method developed recently to enable forced
132 protein granule formation through multivalent interactions[34] (Extended Data Fig. 15). HOtag-

133 induced cytoplasmic granule formation of either the ΔTD or ΔHELP mutants of EML4-ALK
134 locally recruited GRB2 (Fig. 3f, g), increased RAS-GTP levels (Extended Data Fig. 14) and
135 restored RAS/MAPK signaling (Fig. 3h, i). As an important negative control, HOtag-forced
136 clustering of the kinase-deficient EML4-ALK did not promote GRB2 recruitment or
137 RAS/MAPK signaling (Fig. 3f-i and Extended Data Fig. 14). The findings highlight the dual
138 importance of cytoplasmic protein granule formation and intact kinase activity for productive
139 signaling. We also directly tested the role of protein granule formation on cytosolic RAS
140 activation. Compared to wild-type EML4-ALK, the ΔTD mutant that is expressed diffusely in
141 the cytosol demonstrated substantially reduced levels of activated (GTP-bound) cytosolic KRAS-
142 C185S, which could be restored through HOtag-forced clustering (Extended Data Fig. 16).
143 Collectively, our data show that membraneless EML4-ALK cytoplasmic protein granules can
144 spatially concentrate, organize, and initiate RAS/MAPK pathway signaling events.

145 We tested the generality of this model. First, multiple variants of EML4-ALK have been
146 described in cancer patients[18], all comprising the intracellular domain of ALK (but not its
147 transmembrane domain) fused to N-terminal fragments of EML4 of varying lengths (Fig. 4a).
148 We demonstrated that another recurrent form of oncogenic EML4-ALK (variant 3), which
149 contains a further truncation of the TAPE domain but retains the TD[18], also formed cytoplasmic
150 granules that locally recruited GRB2 and increased RAS/MAPK signaling (Fig. 4b-d and
151 Extended Data Figs. 17, 18). In contrast, EML4-ALK variant 5, which lacks the entire TAPE
152 domain of EML4, did not form protein granules and demonstrated significantly less RAS/MAPK
153 signaling compared to the protein granule-forming EML4-ALK variants 1 and 3 (Fig. 4b-d and
154 Extended Data Fig. 18). HOtag-forced clustering of EML4-ALK variant 5 augmented
155 RAS/MAPK signaling (Extended Data Fig. 19). Consistent with the presence of a TD in all
156 EML4-ALK variants, the granule-forming EML4-ALK variants (1 and 3) and the non-granule-
157 forming variant 5 were each capable of self-association in co-immunoprecipitation experiments
158 (Extended Data Fig. 20). These results suggest a functional difference in terms of RAS/MAPK
159 signaling output between higher-order protein granule formation (EML4-ALK variants 1 and 3)
160 and lower-order self-association through oligomerization (EML4-ALK variant 5).

161 Next, as a proof-of-principle for the functional importance of higher-order protein assembly, we
162 engineered an intracellular EGFR (iEGFR) protein lacking the native extracellular and
163 transmembrane domains. This iEGFR is similar to naturally-occurring truncated forms of this
164 RTK and others[35,36] and is distributed diffusely in the cytoplasm and nucleus when expressed
165 alone (Fig. 4e). HOtag forced clustering of iEGFR recruited GRB2 and increased RAS/MAPK
166 signaling in a kinase-dependent manner, analogous to oncogenic ALK (Fig. 4e, f).

167 Finally, we studied another oncogenic RTK, RET, that also undergoes multiple distinct gene
168 rearrangements in human cancer, leading to the elimination of the extracellular and
169 transmembrane domains from the fusion oncoprotein[15]. The recurrent fusion oncoprotein
170 CCDC6-RET formed de novo cytoplasmic protein granules (Fig. 4g, h) which did not
171 demonstrate PM localization or colocalize with intracellular lipid-containing organelles or a
172 lipid-intercalating dye (Extended Data Fig. 21). CCDC6-RET cytoplasmic protein granules
173 recruited GRB2 (Fig. 4h) and locally enriched RAS-GTP as measured by the tandem GFP-RBD
174 reporter (Extended Data Fig. 22a), resulting in increased RAS activation and downstream MAPK
175 signaling (Fig. 4i and Extended Data Fig. 22b, c). Structure-function studies showed that a
176 CCDC6-RET mutant lacking the coiled-coil domain in the CCDC6 component abrogated
177 granule formation (Extended Data Fig. 23) and reduced RAS/MAPK activation (Fig. 4i and

178 Extended Data Fig. 22b, c). A kinase-deficient (K147M) mutant form of CCDC6-RET still
179 formed cytoplasmic protein granules but was unable to recruit GRB2 (Extended Data Fig. 24) or
180 activate RAS/MAPK signaling (Fig. 4i and Extended Data Fig. 22b, c). These results reinforce
181 the dual importance of cytoplasmic protein granules and kinase activity in driving oncogenic
182 RTK/RAS/MAPK signaling. The data also reveal differences between EML4-ALK and CCDC6-
183 RET in the dependence on kinase activity for granule formation.

184 Collectively, our findings show that membraneless cytoplasmic protein granules coordinate RAS
185 activation in a lipid membrane-independent manner in mammalian cells and that de novo
186 formation of these biomolecular condensates may represent a general mechanism for organizing
187 oncogenic kinase signaling in cancer. Oncogenic kinase fusion proteins often contain
188 multimerization domains in the non-kinase fusion partner which are known to be important for
189 self-association and oncogenic signaling[37,38]. However, whether these oncoproteins form
190 condensates and how they spatially coordinate RAS/MAPK signaling have remained open
191 questions. Our results demonstrate that higher-order protein-based assembly in the cytoplasm is
192 one strategy for organizing RTK/RAS/MAPK signaling in cancer. The possibility that similar
193 structures exist in normal cells and the potential interplay between cytoplasmic protein granule-
194 based and canonical lipid membrane-based RTK/RAS/MAPK signaling are areas for future
195 investigation. By deciphering the rules that govern signaling from cytoplasmic protein granules,
196 and factors that influence their formation and stability, new opportunities may emerge for
197 targeted drug development to disrupt protein granules that drive cancer pathogenesis.

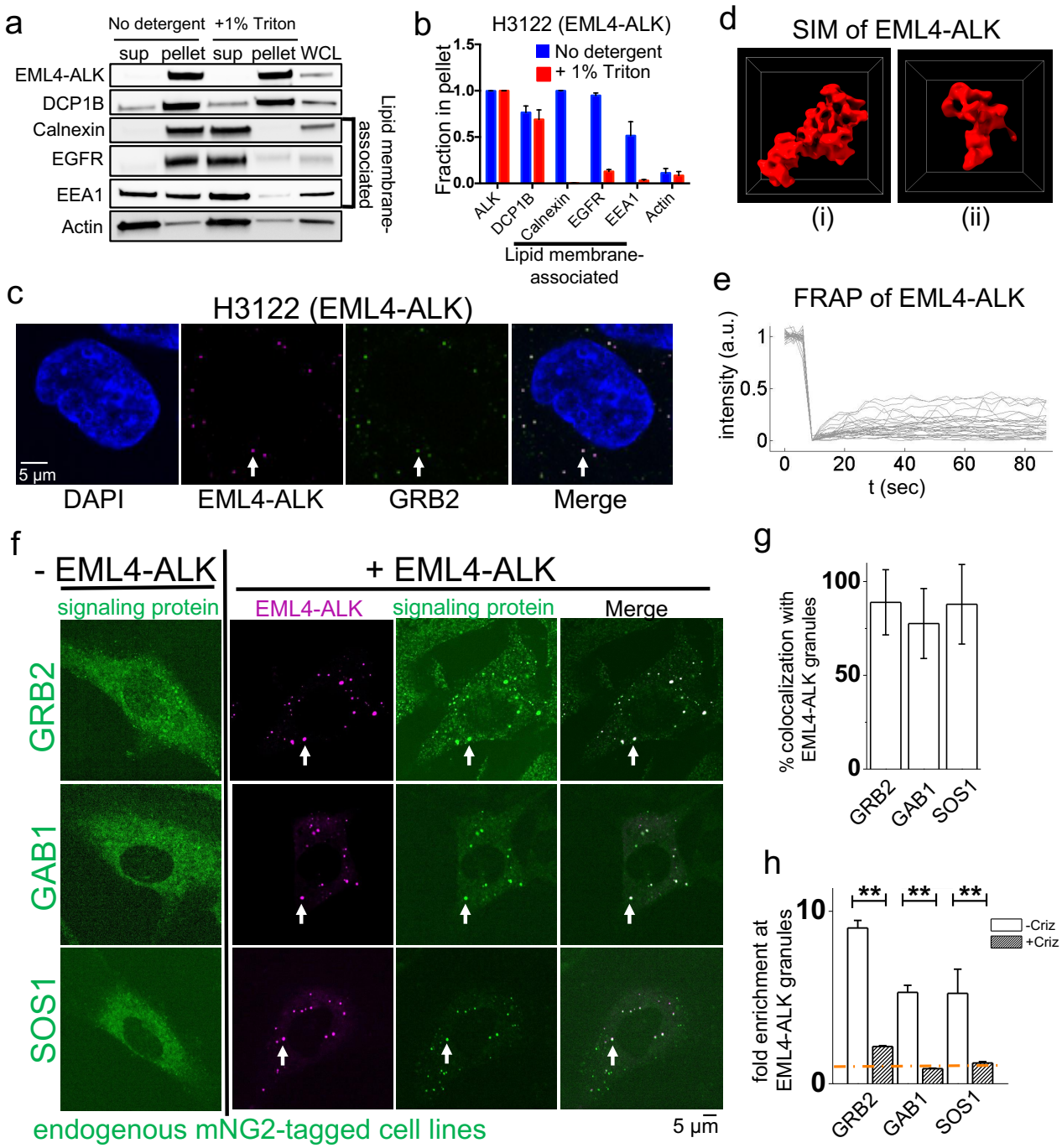

Figure 1: EML4-ALK forms de novo membraneless cytoplasmic protein granules and recruits RAS-activating complex GRB2/SOS1/GAB1 in-situ. a, b, Subcellular fractionation by ultracentrifugation +/– detergent (1% Triton X-100) in EML4-ALK expressing cancer cell line H3122, followed by Western blotting **(a)**. EML4-ALK and DCP1B are statistically distinct ($p < 0.05$, one-way ANOVA) from the lipid membrane-associated proteins, which shift from the insoluble fraction (pellet) to the supernatant (sup) with detergent. Fraction in pellet **(b)** calculated as ratio of the insoluble fraction to total (insoluble plus supernatant fractions) as assessed by

Western blotting, N=3. **c,** Immunofluorescence to detect endogenous expression of EML4-ALK in a patient-derived cancer cell line (H3122) with endogenous mNG2-tagging of GRB2. White arrows indicate a representative EML4-ALK cytoplasmic protein granule with local enrichment of GRB2 (multiple non-highlighted granules also show colocalization between EML4-ALK and GRB2). **d,** SIM images of 2 distinct YFP::EML4-ALK puncta in Beas2B cells. SIM box size: 2 μm × 2 μm × 2 μm. **e,** FRAP analysis of YFP::EML4-ALK expressed in human epithelial cell line Beas2B. Each curve represents photobleaching and recovery of fluorescence intensity for an individual EML4-ALK puncta. N = 30 cells. **f,** Live-cell confocal imaging in Beas2B cells with endogenous mNG2-tagging of GRB2, GAB1, and SOS1 in the presence or absence of mTagBFP2::EML4-ALK. White arrows indicate a representative EML4-ALK cytoplasmic protein granule with local enrichment of respective signaling proteins (multiple non-highlighted granules also show colocalization between EML4-ALK and signaling proteins). **g,** Quantification of colocalization between EML4-ALK granules and relevant signaling proteins. At least 100 total cells were scored in each condition over 3 independent experiments. **h,** Fold-enrichment of signaling proteins at EML4-ALK granules +/– 24 hour treatment with 1 μM Crizotinib (criz). Error bars represent ± SEM, ** $p < 0.01$, paired *t*-test.

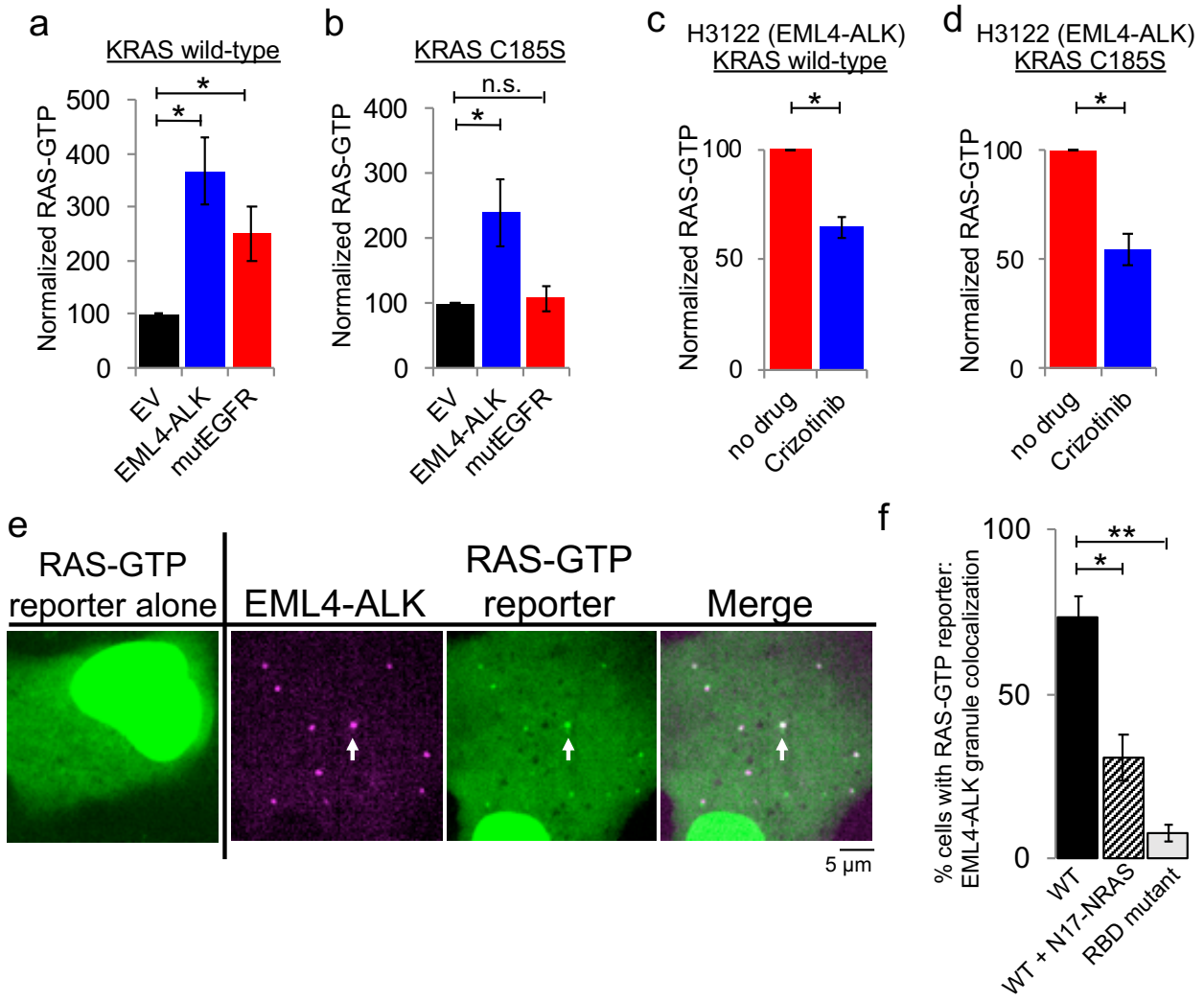

Figure 2: Local RAS activation by cytoplasmic EML4-ALK protein granules. a, b, Stable expression of KRAS wild-type **(a)** or C185S cytosolic mutant **(b)** in 293T cells, followed by transfection of empty vector (EV), EML4-ALK, or oncogenic EGFR. RAS-GTP levels normalized to relevant total RAS species (KRAS wild-type or C185S) and then standardized against EV, N=3. **c, d,** EML4-ALK expressing H3122 cancer cell line with stable expression of KRAS wild-type **(c)** or cytosolic KRAS C185S mutant **(d)** +/– two hours of 100 nM crizotinib. RAS-GTP levels normalized to relevant total RAS species (KRAS wild-type or C185S) and then standardized against DMSO treated H3122 cells (no drug), N=3. **e,** Live-cell confocal imaging of RAS-GTP reporter (tandem GFP-RBD) expressed in human epithelial cell line Beas2B +/- mTagBFP2::EML4-ALK. White arrows indicate a representative EML4-ALK cytoplasmic protein granule with local enrichment of RAS-GTP (multiple non-highlighted granules also show colocalization between EML4-ALK and RAS-GTP reporter). **f,** Quantification of cells with colocalization between RAS-GTP reporter and EML4-ALK granules. WT denotes unmodified tandem GFP-RBD reporter, RBD mutant denotes mutant GFP-RBD reporter (R59A/N64D) with diminished RAS-GTP binding. N = 3 with at least 30 cells per replicate. For all panels, error bars represent ± SEM, * denotes $p < 0.05$, ** $p < 0.01$, n.s. denotes non-significant comparison, one-way ANOVA (a, b, f) or paired *t*-test (c, d).

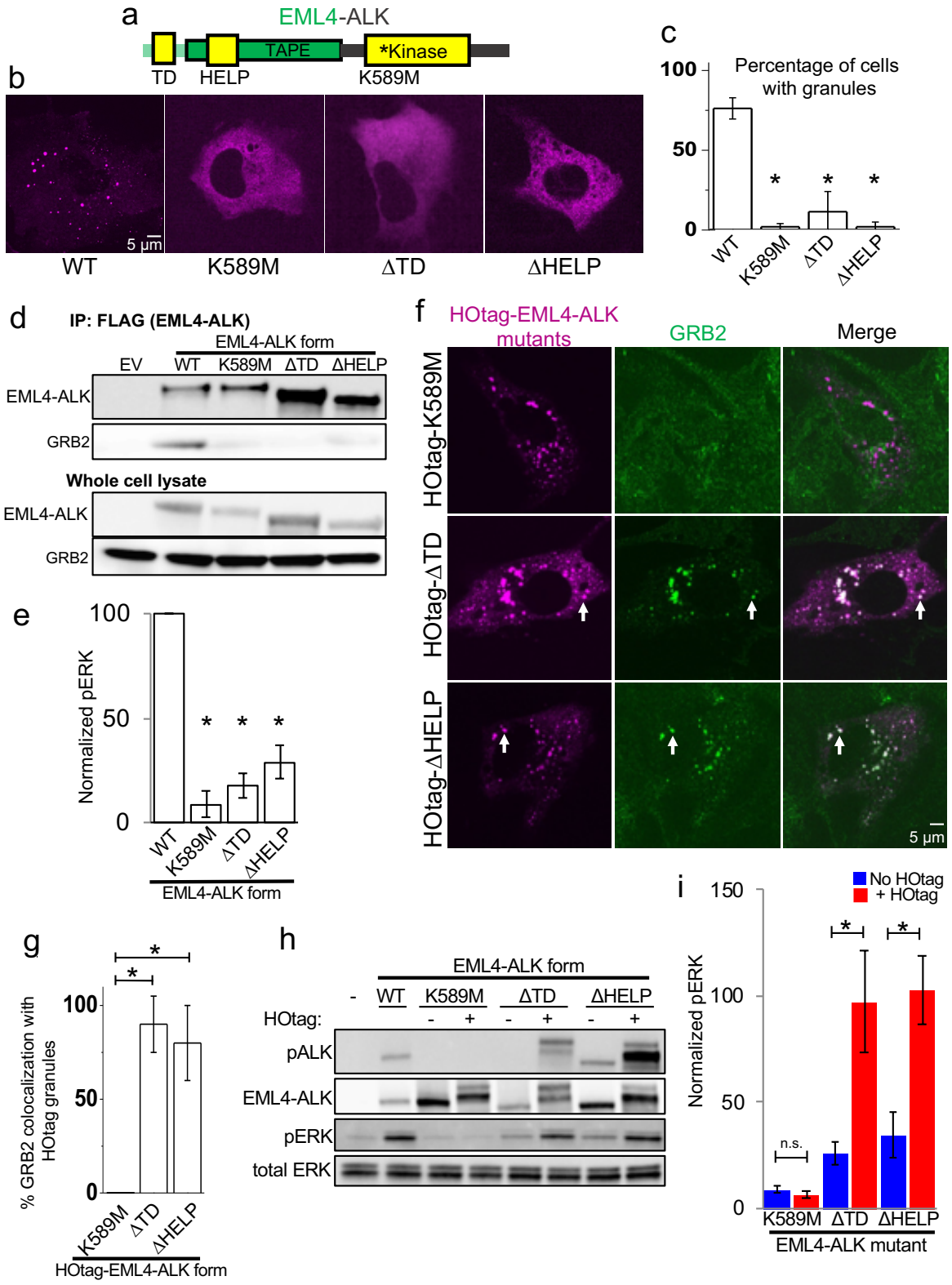

Figure 3: Protein granule formation by EML4-ALK is critical for RAS/MAPK signaling. a, Structure schematic of the EML4-ALK fusion protein with highlighted trimerization domain (TD), hydrophobic EML protein (HELP) motif within the tandem atypical WD-propeller in

EML4 protein (TAPE) domain, and ALK kinase domain. **b,** Live-cell confocal imaging of mTagBFP2::EML4-ALK (denoted as WT for wild-type EML4-ALK) or kinase-deficient (K589M), ΔTD or ΔHELP mutants in human epithelial cell line Beas2B. **c,** Quantification of percentage of cells with granules. At least 75 cells were scored over 3 independent replicates. **d,** Anti-FLAG co-immunoprecipitation of FLAG-tagged wild-type (WT) EML4-ALK or respective mutants expressed in 293T cells, followed by Western blotting to assess GRB2 binding. EV denotes empty vector control, images representative of at least 3 independent experiments. **e,** Quantification of Western blotting upon expression of EML4-ALK or respective mutants in 293T cells. pERK levels were normalized to total ERK and then displayed relative to wild-type EML4-ALK sample which was set to 100, N = 4. **f,** Live-cell confocal imaging of HOtag-mTagBFP2::EML4-ALK ΔTD, ΔHELP, and K589M mutants in Beas2B cells with endogenous mNG2-tagging of GRB2. White arrows indicate representative HOtag-EML4-ALK ΔTD or ΔHELP protein granules with local enrichment of GRB2 (multiple non-highlighted granules also show colocalization between HOtag EML4-ALK mutants and GRB2). **g,** Quantification of percent colocalization between HOtag protein granules of EML4-ALK mutants and GRB2. N = 130 total cells for each condition over 3 independent experiments. **h, i,** Western blotting upon expression of wild-type EML4-ALK or respective mutants +/– HOtag in 293T cells. For quantification, pERK levels were normalized to total ERK and then displayed relative to wild-type EML4-ALK sample which was set to 100, N = 5. For all panels, error bars represent ± SEM, * denotes $p < 0.05$, n.s. denotes non-significant comparison, one-way ANOVA (c, e, g) or paired *t*-test (i).

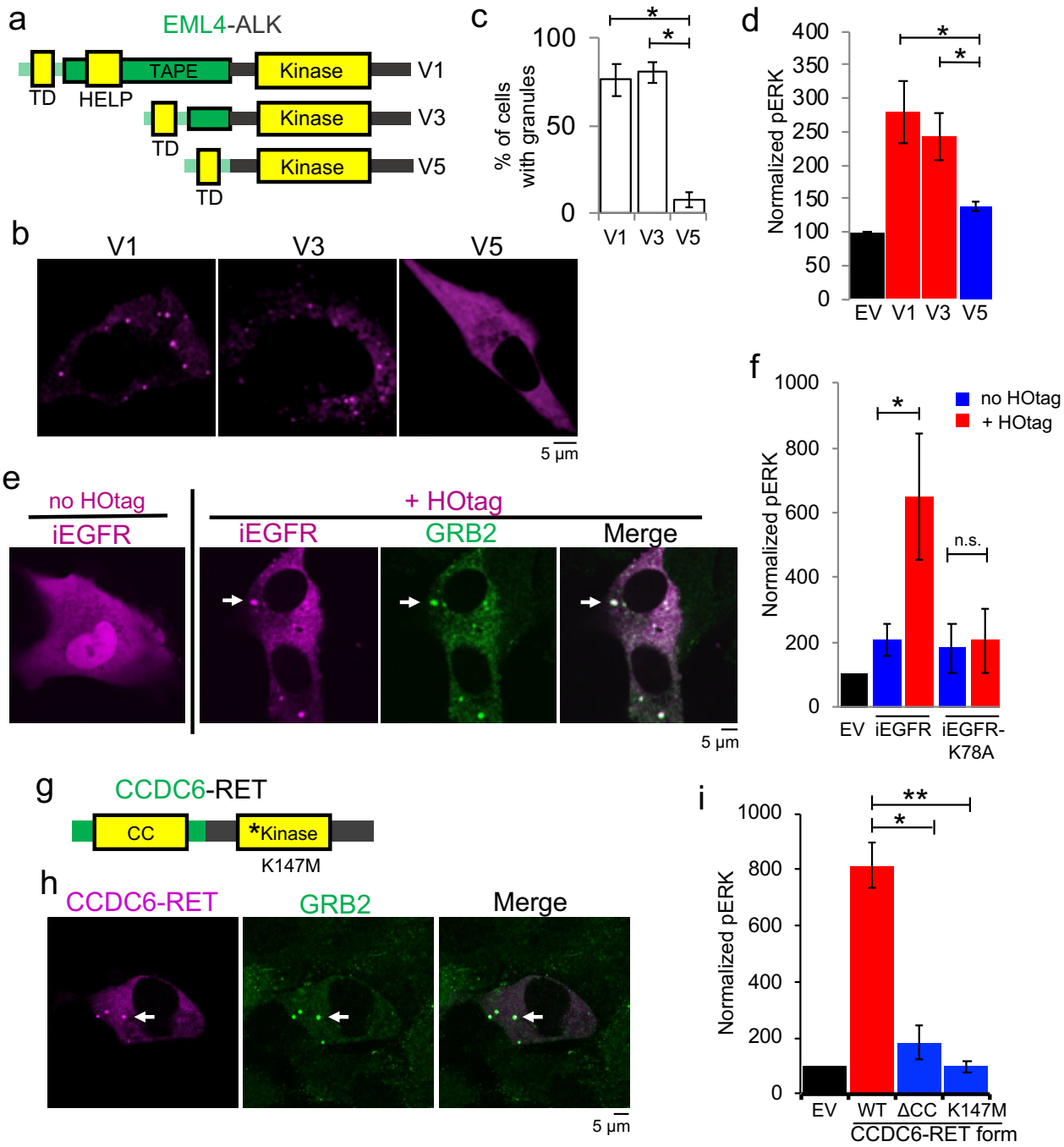

Figure 4: Cytoplasmic granule formation is a mechanism for RTK-mediated RAS/MAPK pathway activation. a, Structure schematic of EML4-ALK fusion protein variants 1, 3, and 5 with highlighted trimerization domain (TD), HELP motif, and TAPE domain. **b,** Live-cell confocal imaging of YFP::EML4-ALK variants 1, 3, and 5 in Beas2B cells. **c,** Quantification of percentage of cells with granules. At least 100 cells were scored over 3 independent replicates. **d,** Quantification of Western blotting results upon expression of EML4-ALK variants or empty vector (EV) in 293T cells. For quantification, pERK levels were normalized to total ERK and then displayed relative to EV sample which was set to 100, N = 3. **e,** Live-cell confocal imaging

of mTagBFP2::iEGFR +/– forced clustering (HOtag) in Beas2B cells with endogenous mNG2-tagging of GRB2. White arrows indicate a representative HOtag-iEGFR protein granule with local enrichment of GRB2 (multiple non-highlighted granules also show colocalization between HOtag-iEGFR and GRB2). **f,** Quantification of Western blotting results upon expression of EV, iEGFR or iEGFR kinase-deficient mutant (iEGFR-K78A) +/– HOtag in 293T cells. For quantification, pERK levels were normalized to total ERK and then displayed relative to EV sample which was set to 100, N = 6. **g,** Structure schematic of the CCDC6-RET fusion protein with CCDC6 coiled-coiled domain (CC) and RET kinase domain. **h,** Live-cell confocal imaging of mTagBFP2::CCDC6-RET in Beas2B cells with endogenous mNG2-tagging of GRB2. White arrows indicate a representative CCDC6-RET cytoplasmic protein granule with local enrichment of GRB2 (multiple non-highlighted granules also show colocalization between CCDC6-RET and GRB2). **i,** Quantification of Western blotting results upon expression of EV, wild-type CCDC6-RET (WT), and CCDC6-RET ΔCC and kinase-deficient (K147M) mutants. For quantification, pERK levels were normalized to total ERK and then displayed relative to EV sample which was set to 100, N=4. All images in this figure are representative of at least 25 analyzed cells in 3 independent experiments. Error bars represent ± SEM, * denotes $p < 0.05$, ** $p < 0.01$, n.s. denotes non-significant comparison, one-way ANOVA.

References:

1 Banani, S. F., Lee, H. O., Hyman, A. A. & Rosen, M. K. Biomolecular condensates: organizers of cellular biochemistry. *Nature Reviews Molecular Cell Biology* **18**, 285-298, doi:10.1038/nrm.2017.7 (2017).

2 Cheng, X. & Smith, J. C. Biological Membrane Organization and Cellular Signaling. *Chemical Reviews* **119**, 5849-5880, doi:10.1021/acs.chemrev.8b00439 (2019).

3 Cox, A. D., Der, C. J. & Philips, M. R. Targeting RAS Membrane Association: Back to the Future for Anti-RAS Drug Discovery? *Clinical cancer research : an official journal of the American Association for Cancer Research* **21**, 1819-1827, doi:10.1158/1078-0432.CCR-14-3214 (2015).

4 Willumsen, B. M., Christensen, A., Hubbert, N. L., Papageorge, A. G. & Lowy, D. R. The p21 ras C-terminus is required for transformation and membrane association. *Nature* **310**, 583-586 (1984).

5 Sanchez-Vega, F. *et al.* Oncogenic Signaling Pathways in The Cancer Genome Atlas. *Cell* **173**, 321-337.e310, doi:10.1016/j.cell.2018.03.035 (2018).

6 Plowman, S. J., Muncke, C., Parton, R. G. & Hancock, J. F. H-ras, K-ras, and inner plasma membrane raft proteins operate in nanoclusters with differential dependence on the actin cytoskeleton. *Proceedings of the National Academy of Sciences* **102**, 15500-15505, doi:10.1073/pnas.0504114102 (2005).

7 Prior, I. A., Muncke, C., Parton, R. G. & Hancock, J. F. Direct visualization of Ras proteins in spatially distinct cell surface microdomains. *J Cell Biol* **160**, 165-170, doi:10.1083/jcb.200209091 (2003).

8 Huang, W. Y. C. *et al.* A molecular assembly phase transition and kinetic proofreading modulate Ras activation by SOS. *Science (New York, N.Y.)* **363**, 1098-1103, doi:10.1126/science.aau5721 (2019).

9 Su, X. *et al.* Phase separation of signaling molecules promotes T cell receptor signal transduction. *Science (New York, N.Y.)* **352**, 595-599, doi:10.1126/science.aad9964 (2016).
10 Shin, Y. & Brangwynne, C. P. Liquid phase condensation in cell physiology and disease. *Science (New York, N.Y.)* **357**, doi:10.1126/science.aaf4382 (2017).
11 Alberti, S., Gladfelter, A. & Mittag, T. Considerations and Challenges in Studying Liquid-Liquid Phase Separation and Biomolecular Condensates. *Cell* **176**, 419-434, doi:10.1016/j.cell.2018.12.035 (2019).
12 Boulay, G. *et al.* Cancer-Specific Retargeting of BAF Complexes by a Prion-like Domain. *Cell* **171**, 163-178.e119, doi:10.1016/j.cell.2017.07.036 (2017).
13 Koken, M. H. *et al.* The t(15;17) translocation alters a nuclear body in a retinoic acid-reversible fashion. *The EMBO journal* **13**, 1073-1083 (1994).
14 Childress, M. A. *et al.* ALK Fusion Partners Impact Response to ALK Inhibition: Differential Effects on Sensitivity, Cellular Phenotypes, and Biochemical Properties. *Molecular cancer research : MCR* **16**, 1724-1736, doi:10.1158/1541-7786.Mcr-18-0171 (2018).
15 Kato, S. *et al.* RET Aberrations in Diverse Cancers: Next-Generation Sequencing of 4,871 Patients. *Clinical Cancer Research* **23**, 1988-1997, doi:10.1158/1078-0432.Ccr-16-1679 (2017).
16 Hrustanovic, G. *et al.* RAS-MAPK dependence underlies a rational polytherapy strategy in EML4-ALK-positive lung cancer. *Nat Med* **21**, 1038-1047, doi:10.1038/nm.3930 (2015).
17 Richards, Mark W. *et al.* Microtubule association of EML proteins and the EML4-ALK variant 3 oncoprotein require an N-terminal trimerization domain. *Biochemical Journal* **467**, 529-536, doi:10.1042/bj20150039 (2015).
18 Sabir, S. R., Yeoh, S., Jackson, G. & Bayliss, R. EML4-ALK Variants: Biological and Molecular Properties, and the Implications for Patients. *Cancers* **9**, 118, doi:10.3390/cancers9090118 (2017).
19 Jackson, J. H. *et al.* Farnesol modification of Kirsten-ras exon 4B protein is essential for transformation. *Proc Natl Acad Sci U S A* **87**, 3042-3046, doi:10.1073/pnas.87.8.3042 (1990).
20 Rizzuto, R., Brini, M., Pizzo, P., Murgia, M. & Pozzan, T. Chimeric green fluorescent protein as a tool for visualizing subcellular organelles in living cells. *Current biology : CB* **5**, 635-642 (1995).
21 Aizer, A. *et al.* The dynamics of mammalian P body transport, assembly, and disassembly in vivo. *Mol Biol Cell* **19**, 4154-4166, doi:10.1091/mbc.E08-05-0513 (2008).
22 Cranfill, P. J. *et al.* Quantitative assessment of fluorescent proteins. *Nature Methods* **13**, 557, doi:10.1038/nmeth.3891 (2016).
23 Patel, A. *et al.* A Liquid-to-Solid Phase Transition of the ALS Protein FUS Accelerated by Disease Mutation. *Cell* **162**, 1066-1077, doi:10.1016/j.cell.2015.07.047 (2015).
24 Molliex, A. *et al.* Phase separation by low complexity domains promotes stress granule assembly and drives pathological fibrillization. *Cell* **163**, 123-133, doi:10.1016/j.cell.2015.09.015 (2015).
25 Kroschwald, S., Maharana, S. & Alberti, S. Hexanediol: a chemical probe to investigate the material properties of membrane-less compartments. *Matters*, doi:10.19185/matters.201702000010 (5-22-2017).

26 Feng, S. *et al.* Improved split fluorescent proteins for endogenous protein labeling. *Nature Communications* **8**, 370, doi:10.1038/s41467-017-00494-8 (2017).
27 Zhou, M. *et al.* VPS35 binds farnesylated N-Ras in the cytosol to regulate N-Ras trafficking. *J Cell Biol* **214**, 445-458, doi:10.1083/jcb.201604061 (2016).
28 Tsao, M.-S. *et al.* Erlotinib in Lung Cancer — Molecular and Clinical Predictors of Outcome. *New England Journal of Medicine* **353**, 133-144, doi:10.1056/NEJMoa050736 (2005).
29 Biskup, C. & Rubio, I. Real-time visualization and quantification of native Ras activation in single living cells. *Methods Mol Biol* **1120**, 285-305, doi:10.1007/978-1-62703-791-4_19 (2014).
30 Rubio, I. *et al.* TCR-Induced Activation of Ras Proceeds at the Plasma Membrane and Requires Palmitoylation of N-Ras. *Journal of immunology (Baltimore, Md. : 1950)* **185**, 3536-3543, doi:10.4049/jimmunol.1000334 (2010).
31 Sigal, I. S. *et al.* Mutant ras-encoded proteins with altered nucleotide binding exert dominant biological effects. *Proceedings of the National Academy of Sciences* **83**, 952-956, doi:10.1073/pnas.83.4.952 (1986).
32 Rai, A. K., Chen, J.-X., Selbach, M. & Pelkmans, L. Kinase-controlled phase transition of membraneless organelles in mitosis. *Nature* **559**, 211-216, doi:10.1038/s41586-018-0279-8 (2018).
33 Monahan, Z. *et al.* Phosphorylation of the FUS low-complexity domain disrupts phase separation, aggregation, and toxicity. *The EMBO journal* **36**, 2951-2967, doi:10.15252/embj.201696394 (2017).
34 Zhang, Q. *et al.* Visualizing Dynamics of Cell Signaling In Vivo with a Phase Separation-Based Kinase Reporter. *Mol Cell* **69**, 334-346.e334, doi:10.1016/j.molcel.2017.12.008 (2018).
35 Liao, H.-J. & Carpenter, G. Regulated Intramembrane Cleavage of the EGF Receptor. *Traffic* **13**, 1106-1112, doi:10.1111/j.1600-0854.2012.01371.x (2012).
36 Ni, C.-Y., Murphy, M. P., Golde, T. E. & Carpenter, G. γ-Secretase Cleavage and Nuclear Localization of ErbB-4 Receptor Tyrosine Kinase. *Science (New York, N.Y.)* **294**, 2179-2181, doi:10.1126/science.1065412 (2001).
37 Du, Z. & Lovly, C. M. Mechanisms of receptor tyrosine kinase activation in cancer. *Molecular Cancer* **17**, 58, doi:10.1186/s12943-018-0782-4 (2018).
38 McWhirter, J. R., Galasso, D. L. & Wang, J. Y. A coiled-coil oligomerization domain of Bcr is essential for the transforming function of Bcr-Abl oncoproteins. *Molecular and cellular biology* **13**, 7587-7595, doi:10.1128/mcb.13.12.7587 (1993).

Acknowledgments:
The authors would like to acknowledge Amit Sabnis, Franziska Haderk and Zoji Bomya for experimental help and manuscript review, Mark Philips, Ignacio Rubio, and Richard Bayliss for generously providing plasmids and manuscript review, and Michael Rosen for scientific input and manuscript review.

Funding: This research project was conducted with support from the National Institutes of Health (R01CA231300 to T.G.B and B.H., U54CA224081, R01CA204302, R01CA211052 and

R01CA169338 to T.G.B, R21GM129652, R01GM124334 and U19CA179512 to B.H), Pew and Stewart Foundations (to T.G.B), the UCSF Marcus Program in Precision Medicine Innovation (to B.H. and T.G.B.), the UCSF Byers Award for Basic Science (to B.H.) and the UCSF Physician-Scientist Scholar Program (to A.T.). B.H. is a Chan Zuckerberg Biohub investigator. A.T. also received financial support from Alex's Lemonade Stand, the St. Baldrick's Foundation, the A.P. Giannini Foundation, the Campini Family Foundation, and the Posey Family Foundation. D.S.N. received support from F30 CA210444-04.

Author Contributions: A.T., J.G., D.S.N., B.H. and T.G.B. designed the study. A.T., J.G., D.S.N., H.L., A.H., H.A., S.P., A.R., X.S., B.Y., S.F. performed experiments, collected and analyzed data. A.T., J.G., D.S.N., B.H. and T.G.B wrote the manuscript. B.H. and T.G.B oversaw the study. All authors have approved the manuscript.

Competing interests: T.G.B. is an advisor to Array Biopharma, Revolution Medicines, Novartis, Astrazeneca, Takeda, Springworks, Jazz Pharmaceuticals, and receives research funding from Novartis and Revolution Medicines.

Data and Materials Availability: All data is available in the main text or the supplementary materials.